[Article] doi: 10.3866/PKU.WHXB2016032807 www.whxb.pku.edu.cn

室温下Kelvin探针力显微镜分析离子液体的界面

张小宁[1,*] 胡红美[2]

([1]Department of Mathematics, Sciences and Technology, Paine College, Augusta 30901, Georgia, USA;
[2]浙江省海洋水产研究所，浙江省海水增养殖重点实验室，浙江 舟山 316021)

摘要：研究离子液体阳离子和阴离子在界面的排列具有意义，因为它们能够影响离子液体在界面的表面结构和属性。作为一种扫描探针显微技术，Kelvin探针力显微镜(KPFM)在本文中被用于室温下离子液体界面性质的研究。离子液体氯化(1-丁基-3-甲基咪唑)([Bmim]Cl)在本文中被用作研究对象。实验中，[Bmim]Cl被选择性地固定在亲液的化学修饰表面，形成超薄的固态吸附层和液滴。由于表面电势能够用于直接指示表面偶极子，因而对于检测分子的取向十分有用。利用KPFM获得的表面电势图表明[Bmim]Cl离子液体在气液界面(当离子液体以液滴形式存在)和气固界面(当离子液体以固态吸附层形式存在)呈现出不同的分子排列。我们的研究表明Kelvin探针力显微镜能够用于表征离子液体在界面的分子排列。

关键词：Kelvin探针力显微镜；氯化(1-丁基-3-甲基咪唑)；表面电势；离子液体的分子排列；界面
中图分类号：O647

Investigation of Interfaces of Ionic Liquid *via* Kelvin Probe Force Microscopy at Room Temperature

ZHANG Xiao-Ning[1,*] HU Hong-Mei[2]

([1]*Department of Mathematics, Sciences and Technology, Paine College, Augusta 30901, Georgia, USA*;
[2]*Key Laboratory of Mariculture and Enhancement of Zhejiang Province, Marine Fishery Institute of Zhejiang Province, Zhoushan 316021, Zhejiang Province, P. R. China*)

Abstract: The alignment of the ionic liquid (IL) cation and anion at the interface is of interest because it would affect the surface structures and properties of IL at the interfaces. In this study, Kelvin probe force microscopy (KPFM), a scanning probe microscopy technique, was used to investigate the interfacial properties of the IL at room temperature. A model molecule, 1-butyl-3-methylimidazolium chloride ([Bmim]Cl), was selectively assembled on the lyophilic chemical patterns prepared on a substrate, forming ultrathin solid-like adsorbate layers and droplets. Because the surface potential is a direct indicator of the surface dipole, which is useful for examining molecular orientation, the surface potential maps captured by KPFM indicated that the [Bmim]Cl molecules demonstrated different orientations at the gas-liquid interface (in the form of a droplet) and at the gas-solid interface (in the form of a solid-like adsorbate layer). Our results indicate that KPFM has potential for the characterization of IL molecular alignment at interfaces.

Key Words: Kelvin probe force microscopy; 1-Butyl-3-methylimidazolium chloride; Surface potential; Ionic liquid molecular arrangement; Interface

Received: December 25, 2015; Revised: March 28, 2016; Published on Web: March 28, 2016.
*Corresponding author. Email: XZhang@paine.edu; Tel: +1-706-821-8384.
The project was supported by the National Science Foundation, USA (HRD-1505197).
美国国家科学基金会(HRD-1505197)资助项目

1 Introduction

Studies have revealed that the improvements of ionic liquid (IL) interfacial properties can be affected by the alignment of IL cations and anions. While the IL surface structures influence adsorption and desorption phenomena as well as mass transport[1], they also influence IL applications in engineering[2], analytical chemistry[3,4], and nanoparticle synthesis[5,6]. Some experimental techniques, such as direct recoil spectrometry[7,8], neutron and X-ray reflectivity[9,10], sum frequency generation vibrational spectroscopy[11], and also photoelectron spectroscopy techniques[12], have been used to understand the surface structure in ionic liquids at the interface, although further complex data analyses are required for those techniques.

As a scanning probe microscopy technique, Kelvin probe force microscopy (KPFM) allows imaging of local sample surface potential. The surface potential is a direct indicator of the surface dipole, which is useful for examing molecular orientation[13,14]. In this paper, KPFM was applied to characterize the surface potential of IL at the interface. IL droplets and IL ultrathin adsorbate layer were specifically adsorbed on the chemically modified surface. The alignment of IL ions at the gas-liquid interface was used to compare against that of IL ions at the gas-solid interface. Our results indicate that the preferential arrangement of the IL ions at the gas-liquid interface is different from that at the gas-solid interface, and KPFM has potential for the characterization of IL molecular arrangement at the interface.

2 Materials and methods

2.1 Materials

Octadecyltrichlorosilane (OTS, 97%) was purchased from Gelest (United States). Toluene (99.8%) was purchased from Fisher Scientific (United States). 1-butyl-3-methylimidazolium chloride ([Bmim]Cl, ≥ 99.0%), sulfuric acid (95%−98%), hydrogen peroxide (30% (*w*)), and ultraflat silicon (100) wafers (N-type) were purchased from Sigma-Aldrich (United States).

2.2 Instrumentation

Surface patterns were fabricated using an Agilent (United States) PicoPlus 3000 atomic force microscope (AFM) in an environmental chamber. MikroMasch (United States) CSC-17/Ti-Pt tips were employed for pattern fabrication. MikroMasch NSC-14 tips (150 kHz resonant frequency) were used in IL-coated chemical patterns′ characterization in alternating current (AC) mode. During imaging, the imaging amplitude set point was varied so that the tip tapped the surface gently. The conducting high-aspect-ratio Ag_2Ga tip (from NaugaNeedles, United States) and Veeco (United States) Multimode AFM (J scanner, working in the surface potential mode) were used for KPFM characterization. The sample was ground. The Ag_2Ga tip was held at 4 nm above the surface, with a 10 V AC amplitude applied on the tip. During KPFM characterization, the topography and surface potential images were acquired simultaneously. All AFM images were processed and rendered using WSxM[15].

2.3 Coating IL on chemical patterns

Silicon (100) wafers were cut into 1 cm × 1 cm pieces. The wafer samples were cleaned by piranha solution (1 part of H_2SO_4 and 2 parts of H_2O_2) at 125 °C for 15 min. After rinsing the samples in deionized water and drying in an ultrapure nitrogen environment, the cleaned samples were immersed in a 5 mmol·L^{-1} OTS toluene solution for 12 h at 25 °C in order to form an OTS film on the sample surface[16].

A Mikromasch-type CSC17 platinum-titanium-coated conductive AFM tip was used in the pattern fabrication process and was connected to the virtual ground. During fabrication, a 5 to 10 V direct current (DC) bias was applied to the OTS coated Si wafer. In this case, the Pt-Ti-coated tip acted as the cathode, and the OTS wafer acted as the anode. Since the voltage applied is higher than the water electrolysis reaction needs (1.23 V), the water between the tip and the sample was electrolyzed, generating active oxygen species such as ozone, atomic oxygen, and hydroxyl radical, which can oxidize the methyl-terminated OTS film to carboxylic acid-terminated patterns. This partially degraded OTS pattern is called an OTSpd pattern[17,18]. Fig.1(a) is a representative topography image of OTSpd patterns. It shows that there are bright spots in the center of the OTSpd patterns. These peaks are SiO_2, which is formed due to the deep oxidation directly under the in-

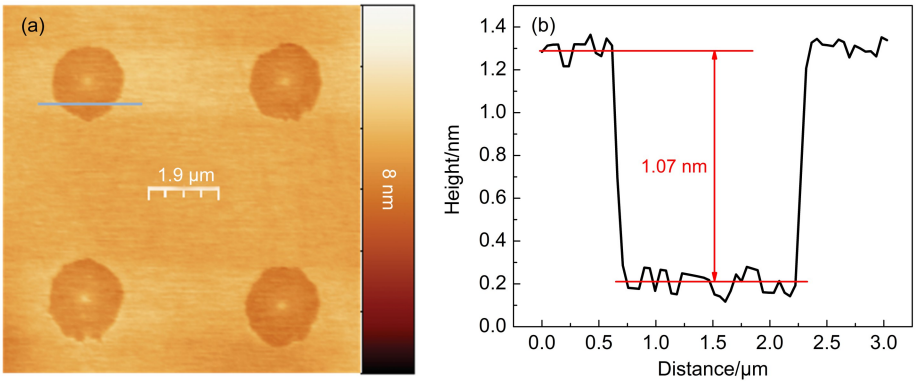

Fig.1 (a) Topography image of an array of octadecyltrichlorosilane (OTS) partially degraded (OTSpd) patterns; (b) topography channel cross-sectional profile, corresponding to the cyan line shown in (a), indicating the depth of the OTSpd disk (1.07 nm) lower than that of the OTS background

tense electric field[19]. The depth of OTSpd measured from the topography channel cross-sectional profile (Fig.1(b)) (1.07 nm) is lower than that of the OTS background.

In a sealed vial, 5 g [Bmim]Cl powder was heated to 120 °C and then cooled to room temperature. After cooling, [Bmim]Cl in the vial existed as a viscous super-cooled liquid at 25 °C. A drop of liquid [Bmim]Cl was then placed on the newly prepared OTSpd pattern area for 1 min, and a pipette was used to remove the IL drop from the sample surface. The OTSpd pattern is a high energy, lyophilic surface whereas the OTS background is a methyl-terminated, low energy, lyophobic surface. Based on the wetting-driven assembly approach[20], IL can be only assembled on the OTSpd patterns due to the contrast in surface energy[21,22]. Two types of patterns associated with ionic liquid can be formed, including ultrathin interfacial IL layers adsorbed on OTSpd discs (Scheme 1, (a) → (b)), as well as IL droplets assembled on the OTSpd discs (Scheme 1, (a) → (c)). These two types of patterns are intermixed with each other on the sample surface. Since [Bmim]Cl is miscible with water, when the sample surface with IL adsorbate layers/droplets was immersed in water, all the materials on the OTSpd disc areas disappeared, indicating that the substances assembled on the OTSpd patterns were [Bmim]Cl.

3 Results and discussion

A Vecco Multimode AFM was used to perform surface potential measurements. KPFM maps the surface potential distribution over the surface, which could provide information in the preferential arrangement of the IL ions at the interface[23]. [Bmim]Cl was studied in this report because [Bmim]Cl has large viscosity compared with other ionic liquids.

As Fig.2 demonstrates, the height of the IL adsorbate layer on the OTSpd pattern (0.46 nm) is higher than that of the OTS background. Since the OTSpd pattern is 1.07 nm below the OTS background, the actual thickness of the IL adsorbate layer can be calculated as 1.53 nm. In the surface potential channel cross-sectional profile (blue line in Fig.2(c), the surface potential over the ultrathin IL adsorbate layer has a value of 10 mV higher than that of the OTS background. Since IL does not adsorb on the low-energy OTS surface, the surface potential of methyl terminated OTS film can be used as an internal reference for comparison of the surface properties of the OTSpd-IL patterns.

In the work of Yokota *et al.*[24], flat substrates of highly ordered pyrolytic graphite (HOPG) and mica were immersed under ILs, and the solid-like layered structure at ionic liquid/substrates interface was observed directly *via* AFM. It is believed that beyond

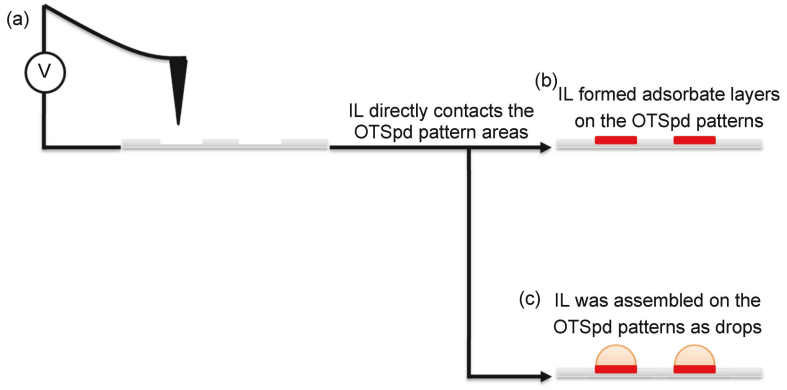

Scheme 1 Preparation of OTSpd patterns on the OTS surface and subsequent 1-butyl-3-methylimidazolium chloride ([Bmim]Cl) adsorption on the OTSpd patterns

(a) fabrication of OTSpd patterns on the OTS film using atomic force microscope (AFM) deep oxidation lithography. [Bmim]Cl in liquid phase was placed on the OTSpd pattern area and selectively assembled on the lyophic OTSpd patterns, forming ultrathin ionic liquid (IL) adsorbate layers (b) and IL droplets (c).

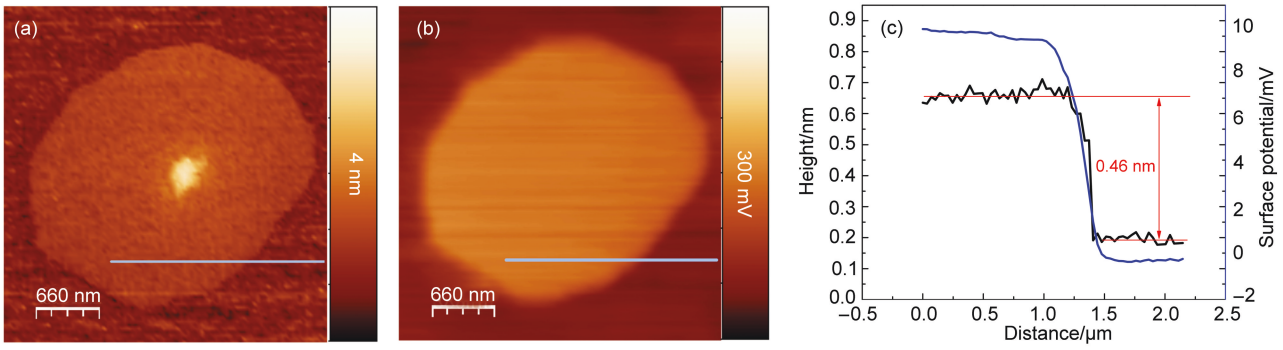

Fig.2 (a) Topography image of the [Bmim]Cl ultrathin adsorbate layer coated on the OTSpd pattern; (b) surface potential map corresponding to the topography image in (a); (c) topography (black line) and surface potential (blue line) channel cross-sectional profiles corresponding to the cyan lines shown in (a) and (b)

color online

this solid-like thin layer, the ionic liquid adopts essentially the bulk structure (in liquid phase)[25]. Our observation is consistent with those studies. Fig.3(a) is a representative AFM topography image, which shows an IL droplet sitting on an IL adsorbate layer that was bound on the carboxylic acid-terminated OTSpd surface. Although the color contrast difference between the OTS background and the IL adsorbate can be barely observed in AFM topography image due to the small height difference between the OTS background and the IL adsorbate layer with a 260 nm color scale, the height cross-sectional profile, corresponding to the cyan line in Fig.3(a) indicating that the height of the IL adsorbate layer is 0.47 nm, which is consistent with the height value observed in Fig.2. In addition, from the AFM phase image (Fig.3(b)), the phase contrast difference among the IL adsorbate layer, IL droplet, and the OTS background can be clearly observed revealing that they have different chemical properties. Therefore, from both AFM topography and phase signals, we can conclude that if the IL droplet is formed by using approach demonstrated in Scheme 1 (a → c), it sits on the IL adsorbate layer that is bound the OTSpd surface instead of contacting the OTSpd substrate directly.

During AFM probe scanning, the amplitude set point led to the AFM tip tap on the IL and interacted with the IL. Both topography and phase signal oscillations in Fig.3 were observed when the tip scanned over the droplet. The oscillation indicates that the droplet was still fluidic. In comparison, under the same amplitude set point, the AFM scan lines over the IL adsorbate layer and the OTS film background, in both Fig.2 and Fig.3, did not show any oscillation because both of the IL adsorbate layer and the OTS film background were in solid phase. Because IL adsorbate layers demonstrated in Fig.2 and Fig.3 are in solid phase, and both of them possess a same topography height above the OTS background, it is able for us to conclude that both IL adsorbate layer shown in Fig.2 and Fig.3 have the same surface characteristics including the surface potential feature.

Fig.4(a) shows another representative IL drop adsorbed on an OTSpd pattern *via* route (a) → (c) (Scheme 1), appearing as a white bump. Fig.4(b) is the surface potential map of the IL drop corresponding to Fig.4(a). On the surface potential map, the brighter area corresponds to a larger work function; therefore, the work function on the IL drop is much smaller than the supporting material, methyl terminated OTS surface. As shown in the cross-sectional profile (Fig.4(c)), the [Bmim]Cl droplet has a surface potential of −480 mV and a height value of 24 nm with respect to the OTS background. The surface potential map provides us information that the arrangement of IL cations and anions at the gas-liquid interface is transformed compare to that at the gas-solid interface (IL adsorbate layer on the OTSpd pattern discs). This experimental result is consistent with Cremer's work[1], in which the

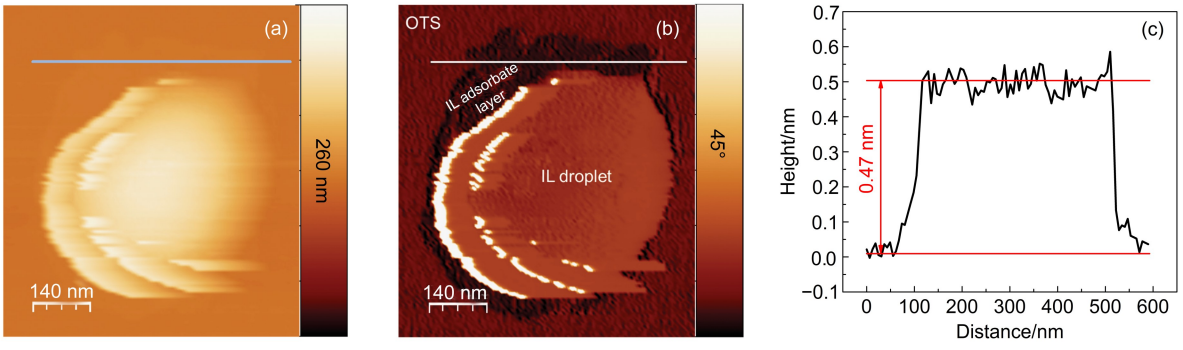

Fig.3 IL droplet sits on the OTSpd pattern (a, b) and height cross-sectional profile (c)

(a) topography image of a [Bmim]Cl droplet on OTSpd. (b) phase image corresponding to the topography image in (a). The phase signals are different for the IL adsorbate layer, IL droplet, and OTS background. Therefore, they have different surface structure. (c) Height cross-sectional profile shows that the IL adsorbate layer underneath the IL droplet is 0.47 nm higher than the OTS background. color online

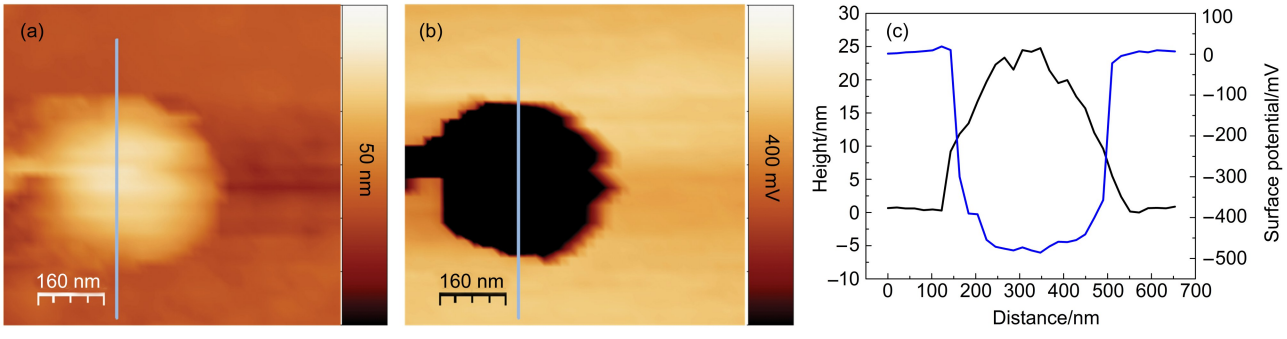

Fig.4 (a) Topography image of the [Bmim]Cl IL droplet assembled on the OTSpd pattern; (b) surface potential map corresponding to the topography image in (a); (c) topography (black line) and surface potential (blue line) channel cross-sectional profiles corresponding to the cyan lines shown in (a) and (b)

color online

arrangement of IL ions on Ni(111) transformed when increasing the IL surface coverage.

4 Conclusions

In this paper, the alignment of [Bmim]Cl ions at interfaces such as those of a gas-liquid and a gas-solid has been investigated by using KPFM. The study demonstrated that KPFM can be used as a tool to reveal the molecular arrangement of IL at an interface. It is hoped that this study can provide experimental data for further theoretical studies. Future directions should include exploring more varieties of ionic liquids *via* KPFM and combine this approach with other techniques, such as sum frequency generation[23] or photoelectron spectroscopy[12], to identify more precise arrangements and structures of ionic liquids at their interfaces.

References

(1) Cremer, T.; Wibmer, L.; Calderon, S. K.; Deyko, A.; Maier, F.; Steinruck, H. P. *Phys. Chem. Chem. Phys.* **2012,** *14*, 5153. doi: 10.1039/C2CP40278E

(2) Werner, S.; Haumann, M.; Wasserscheid, P. *Annu. Rev. Chem. Biomol. Eng.* **2010,** *1*, 203. doi: 10.1146/annurev-chembioeng-073009-100915

(3) Anderson, J. L.; Armstrong, D. W.; Wei, G. T. *Anal. Chem.* **2006,** *78*, 2892. doi: 10.1021/ac069394o

(4) Sun, P.; Armstrong, D. W. *Anal. Chim. Acta* **2010,** *661*, 1. doi:10.1016/j.aca.2009.12.007

(5) Höfft, O.; Endres, F. *Phys. Chem. Chem. Phys.* **2011,** *13*, 13472. doi: 10.1039/C1CP20501C

(6) Dupont, J.; Scholten, J. D. *Chem. Soc. Rev.* **2010,** *39*, 1780. doi: 10.1039/B822551F

(7) Gannon, T. J.; Law, G.; Watson, P. R.; Carmichael, A. J.; Seddon, K. R. *Langmuir* **1999,** *15*, 8429. doi: 10.1021/la990589j

(8) Law, G.; Watson, P. R.; Carmichael, A. J.; Seddon, K. R. *Phys. Chem. Chem. Phys.* **2001,** *3*, 2879. doi: 10.1039/B101952J

(9) Bowers, J.; Vergara-Gutierrez, M. C.; Webster, J. R. P. *Langmuir* **2003,** *20*, 309. doi: 10.1021/la035495v

(10) Sloutskin, E.; Ocko, B. M.; Tamam, L.; Kuzmenko, I.; Gog, T.; Deutsch, M. *J. Am. Chem. Soc.* **2005,** *127*, 7796. doi: 10.1021/ja0509679

(11) Baldelli, S. *J. Phys. Chem. B* **2003,** *107*, 6148. doi: 10.1021/jp027753n

(12) Lovelock, K. R.; Villar-Garcia, I. J.; Maier, F.; Steinrück, H. P.; Licence, P. *Chem. Rev.* **2010,** *110*, 5158. doi: 10.1021/cr100114t

(13) Lü, J.; Delamarche, E.; Eng, L.; Bennewitz, R.; Meyer, E.; Güntherodt, H. J. *Langmuir* **1999,** *15*, 8184. doi: 10.1021/la9904861

(14) Hubbard, A. T. *The Handbook of Surface Imaging and Visualization*; CRC Press: New York, 1995; pp 23−31.

(15) Horcas, I.; Fernandez, R.; Gomez-Rodriguez, J. M.; Colchero, J.; Gomez-Herrero, J.; Baro, A. M. *Rev. Sci. Instrum.* **2007,** *78*, 013705. doi: 10.1063/1.2432410

(16) Trajkovic, S.; Zhang, X.; Daunert, S.; Cai, Y. *Langmuir* **2011,** *27*, 10793. doi: 10.1021/la2016885

(17) Zhang, X. N.; Cai, Y. G. *Beilstein J. Nanotechnol.* **2012,** *3*, 33. doi: 10.3762/bjnano.3.4

(18) Cai, Y.; Lu, L. The Scanning Probe-Based Deep Oxidation Lithography and Its Application in Studying the Spreading of Liquid *N*-Alkane. In *Scanning Probe Microscopy in Nanoscience and Nanotechnology 2*; Springer: Heidelberg, 2011; pp 385−413.

(19) Cai, Y. *Langmuir* **2009,** *25*, 5594. doi: 10.1021/la9004483

(20) Chowdhury, D.; Maoz, R.; Sagiv, J. *Nano Lett.* **2007,** *7*, 1770. doi: 10.1021/nl070842x

(21) Lu, L.; Cai, Y. *Langmuir* **2009,** *25*, 13914. doi: 10.1021/la9016917

(22) Lu, L.; Zander, K. J.; Cai, Y. *Langmuir* **2010,** *26*, 5624. doi: 10.1021/la904387d

(23) Martinez, I. S.; Baldelli, S. *J. Phys. Chem. C* **2010,** *114*, 11564. doi: 10.1021/jp1039095

(24) Yokota, Y.; Harada, T.; Fukui, K. I. *Chem. Commun.* **2010,** *46*, 8627. doi: 10.1039/C0CC02643C

(25) Baldelli, S. *Acc. Chem. Res.* **2008,** *41*, 421. doi: 10.1021/ar700185h